

# UC Irvine

## UC Irvine Previously Published Works

### Title

Use of laser tweezers to analyze sperm motility and mitochondrial membrane potential

### Permalink

<https://escholarship.org/uc/item/54s0m6s6>

### Journal

Journal of Biomedical Optics, 13(1)

### ISSN

1083-3668

### Authors

Nascimento, Jaclyn M

Shi, Linda Z

Chandsawangbhuwana, Charlie

et al.

### Publication Date

2008

### DOI

10.1117/1.2839051

### Copyright Information

This work is made available under the terms of a Creative Commons Attribution License, available at <https://creativecommons.org/licenses/by/4.0/>

Peer reviewed



Published in final edited form as:

*J Biomed Opt.* 2008 ; 13(1): 014002. doi:10.1117/1.2839051.

## Use of laser tweezers to analyze sperm motility and mitochondrial membrane potential

**Jaclyn M. Nascimento,**

University of California, San Diego, Department of Electrical and Computer Engineering, 9500 Gilman Drive, La Jolla, California 92093, jaclyn.nascimento@gmail.com

**Linda Z. Shi,**

University of California, San Diego, Department of Bioengineering, 9500 Gilman Drive, La Jolla, California 92093

**Charlie Chandsawangbhuwana,**

University of California, San Diego, Department of Bioengineering, 9500 Gilman Drive, La Jolla, California 92093

**James Tam,**

University of California, San Diego, Department of Bioengineering, 9500 Gilman Drive, La Jolla, California 92093

**Barbara Durrant,**

Zoological Society of San Diego, San Diego, Beckman Center for Conservation and Research for Endangered Species, 15600 San Pasqual Valley Road, Escondido, California 92027

**Elliot L. Botvinick, and**

University of California, Irvine, Beckman Laser Institute, 1002 Health Sciences Road, Irvine, California 92612

**Michael W. Berns**

University of California, Irvine, Beckman Laser Institute, 1002 Health Sciences Road, Irvine, California 92612 and University of California, San Diego, 9500 Gilman Drive, La Jolla, California 92093

### Abstract

We combine laser tweezers with custom computer tracking software and robotics to analyze the motility [swimming speed, VCL (curvilinear velocity), and swimming force in terms of escape laser power (Pesc)] and energetics [mitochondrial membrane potential (MP)] of individual sperm. Domestic dog sperm are labeled with a cationic fluorescent probe, DiOC<sub>2</sub>(3), that reports the MP across the inner membrane of the mitochondria located in the sperm's midpiece. Individual sperm are tracked to calculate VCL. Pesc is measured by reducing the laser power after the sperm is trapped using laser tweezers until the sperm is capable of escaping the trap. The MP is measured every second over a 5-s interval during the tracking phase (sperm is swimming freely) and continuously during the trapping phase. The effect of the fluorescent probe on sperm motility is addressed. The sensitivity of the probe is measured by assessing the effects of a mitochondrial uncoupling agent (CCCP) on MP of free swimming sperm. The effects of prolonged exposure to the laser tweezers on VCL and MP are analyzed. The system's capabilities are demonstrated by

measuring VCL, Pesc, and MP simultaneously for individual sperm. This combination of imaging tools is useful to quantitatively assess sperm quality and viability.

## Keywords

sperm motility; laser tweezers; escape laser power; mitochondrial membrane potential; 3,3'-diethyloxycarbocyanine iodide; carbonyl cyanide 3-chlorophenylhydrazine

## 1 Introduction

Quantitative and objective techniques are important for assessing sperm quality. Computer-assisted sperm analysis (CASA) systems have been developed to measure parameters such as curvilinear velocity (VCL), amplitude of lateral head movement, and percent of motile sperm, providing quantitative information about the overall motility of a sperm population.<sup>1,2</sup> In addition, flow cytometry in combination with fluorescent probes has been used to monitor mitochondrial membrane potential (MP) in sperm cells.<sup>3-6</sup> MP, given by the Nernst equation, is dependent on the distribution of hydrogen protons across the inner mitochondrial membrane. This electrochemical proton gradient drives the synthesis of ATP that is used for energy by the cell. Therefore, the fluorescence intensity of cyanine dyes, such as 3,3'-diethyloxycarbocyanine iodide [DiOC<sub>2</sub>(3)], which increases as the magnitude of MP increases, is an indicator of the energetic state of the cell. Studies have demonstrated that high MP in sperm correlates with increased motility<sup>3</sup> as well as high-fertility performance.<sup>4-6</sup> Several fluorescent probes are available, and comparisons between probes have been performed.<sup>4,7</sup> Specifically, Novo et al.<sup>7</sup> showed that the ratiometric technique for estimation of MP using DiOC<sub>2</sub>(3) was an accurate indicator of bacterial MP.

Single spot, gradient force laser tweezers is another tool that has been used to study sperm motility by measuring sperm swimming force. It has been shown<sup>8</sup> that the minimum laser power needed to hold a sperm in the optical trap (threshold escape power) is directly proportional to the sperm's swimming force ( $F=Q \times P/c$ , where  $F$  is the swimming force in Newtons,  $P$  is the laser power in Watts,  $c$  is the speed of light in the medium with a given index of refraction, and  $Q$  is the geometrically determined trapping efficiency parameter). Previous studies have demonstrated a positive correlation between sperm swimming speed and escape laser power.<sup>9-11</sup> Optical traps have also been used<sup>12</sup> in combination with the fluorescent probe JC-1 (5,5', 6,6'-tetra-chloro-1,1', 3,3'-tetraethylbenzimidazolyl-carbocyanine iodide). That study measured MP as the sperm were held in the laser trap. A major drawback, however, was the inability to determine not only the mitochondrial MP of the individual sperm before or after it was exposed to the laser tweezers, but also the sperm's swimming speed and/or swimming force.

Recently, computer tracking software and robotics were combined with the laser tweezers system to automate sperm trapping experiments.<sup>13,14</sup> This custom-designed real-time, automated, tracking and trapping system, or RATTs, presents itself as a potentially useful tool, in addition to CASA systems and flow cytometry, to assist in overall sperm quality assessment. RATTs has been modified to measure mitochondrial MP (prior to, during, and after trapping) in conjunction with swimming speed and escape laser power of individual sperm.<sup>15</sup>

In this paper, we describe the modification of RATTs to analyze domestic dog sperm labeled with the fluorescent probe DiOC<sub>2</sub>(3). The effects of the probe on sperm motility are studied. The probe's, as well as the system's, ability to monitor changes in MP is quantified. The effects of prolonged exposure to the laser tweezers on VCL and MP are analyzed.

Finally, the system's capabilities are demonstrated by simultaneously measuring VCL, *Pesc* (swimming force in terms of escape laser power), and MP for individual sperm. The results show that the combination of laser tweezers, robotics, and the measurement of mitochondrial MP creates a system that is capable of providing a detailed description of individual sperm, including both motility and energetic.

## 2 Materials and Methods

### 2.1 Specimen

Semen samples collected from several domestic dogs were cryogenically frozen according to a standard protocol.<sup>16,17</sup> Studies on human sperm have shown that properly freezing, storing, and thawing sperm has no significant effect on escape force.<sup>18</sup> Furthermore, we compared frozen-thawed and fresh dog sperm from the same semen sample and found that the swimming speed and escape laser power distributions were statistically the same (swimming speed:  $P > 0.06$ ; escape power:  $P > 0.9$ , data not shown). Therefore, frozen-thawed semen samples in this study are considered comparable to fresh samples.

For each experiment, a sperm sample is thawed in a water bath (37 °C) for approximately 1 min and its contents are transferred to an Eppendorf centrifuge tube. The sample is centrifuged at 2000 rpm for 10 min (the centrifuge tip radius is 8.23 cm). The supernatant is removed and the remaining sperm pellet is suspended in 1 mL of pre-warmed media [1 mg of bovine serum albumin (BSA) per 1 mL of Biggers, Whittens, and Whittingham (BWW), osmolality of 270 to 300 mmol/kg water,<sup>19</sup> pH of 7.2 to 7.4]. Note that this media is non-capacitating, as it has a low concentration of bicarbonate<sup>20</sup> (4 mM). Therefore, the sperm do not achieve hyperactivity.

To monitor the voltage potential across the inner membrane of the mitochondria, sperm are labeled with DiOC<sub>2</sub>(3) (3,3'-dithyloxacarbocyanine, 30 nM final dye concentration, Molecular Probes, Invitrogen Corp., Carlsbad, California). DiOC<sub>2</sub>(3) is a cationic cyanine dye that primarily accumulates in the mitochondria of a cell in response to the electrochemical proton gradient, or MP. The probe emits both a red and green fluorescence. The ratiometric parameter (red/green intensity) is a size-independent measure of MP, as the green fluorescence varies with size and red fluorescence is dependent<sup>21</sup> on both size and MP. After the dye is added, the cells are incubated for 20 min in a 37 °C water bath and then centrifuged for 10 min (2000 rpm). The pellet is suspended in the media by "flicking" the tube according to the protocol for the MitoProbe assay kit (Invitrogen Corp.) for flow cytometry. To test sensitivity of both the probe and the system to changes in MP (see Sec. 2.4), an aliquot of sperm are exposed to the proton ionophore CCCP (carbonyl cyanide 3-chlorophenylhydrazone, 50 μM final concentration, Molecular Probes, Invitrogen Corp., Carlsbad, California), which is known<sup>7,22</sup> to decrease the magnitude of the MP. CCCP and DiOC<sub>2</sub>(3) are added to the sperm simultaneously.

Final dilutions of ~30,000 sperm/mL of media are used in the experiments. The sperm dilution is loaded into a 3 mL Rose tissue culture chamber and mounted into a microscope stage holder according to previously described methods.<sup>23</sup> The sample is kept at 37 °C using an air curtain incubator (NEVTEK, ASI 400 Air Stream Incubator, Burnsville, Virginia). A thermocouple is attached to the Rose chamber to ensure temperature stability.

### 2.2 Hardware, Software, and Optical Design

The optical system, shown in Fig. 1(a), is adapted after Nascimento, et al.<sup>10</sup> A single point gradient trap is generated using an Nd:YVO<sub>4</sub> continuous wave 1064-nm wavelength laser (Spectra Physics, BL-106C, Mountain View, California), coupled into a Zeiss Axiovert

S100 microscope equipped with a phase III, 40 $\times$ , 1.3 numerical aperture (NA), oil immersion objective (Zeiss, Thornwood, New York). The laser power in the specimen plane is attenuated by rotating the polarizer, which is mounted in a stepper-motor-controlled rotating mount (Newport Corporation, Model PR50PP, Irvine, California).

The imaging setup, shown in Fig. 1(b), was adapted after Mei et al.<sup>12</sup> Two dual video adapters are used to incorporate the laser into the microscope and simultaneously image the sperm in phase contrast and fluorescence. The laser beam enters the side port of the first dual video adapter and is transmitted to the microscope. A filter (Chroma Technology Corp., Model E700SP-2P, Rockingham, Vermont) is used to prevent back reflections of IR laser light from exiting the top port of the adapter but allow reflected visible light coming from the specimen to pass to the second video adapter. The specimen is viewed in phase contrast using red light filtered from the halogen lamp (Chroma Technology Corp., Model D680/60 X) and in fluorescence using the arc lamp (Zeiss FluoArc). The fluorescence filter cube contains an HQ 500/20-nm excitation filter and a dichroic beamsplitter with a 505-nm cut-on wave-length. The second dual video adapter attached to the top port of the first video adapter uses a filter cube to separate the phase information (reflects >670 nm) from the fluorescence (transmits 500 to 670 nm). The phase contrast images are filtered through a filter (Chroma Technology Corp., Model HQ 675/50M) and acquired by a CCD camera (Cohu, Model 7800, San Diego, California, operating at 40 frames/s) coupled to a variable zoom lens system (0.33 to 1.6 $\times$  magnification) to increase the field of view. For the fluorescent images, a Dual-View system (Optical-Insights, Tucson, Arizona) splits the red and green fluorescent light emitted by the specimen to produce a copy of the image for each color. Fluorescent emission filters are placed in this emission-splitting system (green fluorescence emitter: HQ 535/40-nm M filter; red fluorescence emitter: HQ 605/50-nm M filter, Chroma Technology Corp.). The Dual-View system is coupled to a digital camera (Quantix 57, Roper Scientific Inc., Tucson, Arizona) that captures the fluorescent images.

The hardware and software to perform the experiments in this paper are described in greater detail elsewhere.<sup>15</sup> Briefly, two computers are networked together. An upper-level computer that acquires and displays the images from the Cohu CCD is responsible for tracking and trapping the sperm of interest. The lower-level computer is prompted by the upper-level computer to acquire the fluorescent images of the sperm's mitochondria from the Quantix CCD. From the image, the lower level computer calculates the ratio (red/green) value.

Once the user selects the sperm of interest, the upper level computer tracks the sperm and calculates the VCL (in micrometers per second) in real time. Note that other motility parameters including lateral head movement, straight line velocity, and smoothed-path velocity that are typical of a CASA system are also calculated.<sup>10,13,14</sup> Nascimento et al. found that several of these parameters had near equal influence on the variability in the data set.<sup>10</sup> Therefore, for the purpose of this paper, only VCL is used to describe sperm swimming speed, as it is a more comprehensive parameter, accounting for both forward progression and lateral head movement.<sup>11</sup> During this tracking phase, the microscope stage moves the sperm to the center of the field of view if it nears the edge. In addition, the sperm is relocated to a defined ( $x$ ,  $y$ ) coordinate every second and a command is sent to the lower-level computer to acquire a fluorescent image. For track-and-trap experiments, the sperm is relocated to the laser trap coordinates after being tracked and fluorescently imaged for 5s. Once the sperm is successfully trapped by the laser tweezers, the lower-level computer continuously acquires fluorescent images. Laser power is either kept constant (see Sec. 2.5) or is attenuated (see Sec. 2.6). If the power is attenuated, the power at which the sperm is capable of escaping the trap (Pesc, in milliwatts) is recorded by the upper-level computer. The sperm is tracked and fluorescently imaged for an additional 5s once it is released from or escapes the optical trap. Data for each tracked sperm, including ( $x$ ,  $y$ ) trajectory

coordinates in the field of view, stage movement, instantaneous VCL, and average VCL, for each time point is saved to a file on the upper-level computer. The fluorescent data—including the average, maximum, and minimum ratio values—for each image are saved to a file on the lower-level computer.

### 2.3 Effect of Probe on Sperm Motility

The effects of DiOC<sub>2</sub>(3) on sperm motility are assessed. The swimming speed (VCL in micrometers per second) distribution of sperm exposed to DiOC<sub>2</sub>(3) is compared to that of sperm not exposed to the probe (control). Sperm from each group are analyzed during the same time intervals. During the first time interval, both groups are viewed in phase contrast microscopy only. During the second time interval, again, both groups are viewed in phase contrast microscopy. However, the test group exposed to DiOC<sub>2</sub>(3) are also illuminated with excitation light (500 nm) from the arc lamp.

### 2.4 Sensitivity to Changes in MP

The ability to measure changes in MP as well as the ability to detect and report changes in MP is tested. The test sperm group are exposed to both CCCP (50 μM) and DiOC<sub>2</sub>(3) (30 nM), whereas the control sperm group are labeled only with DiOC<sub>2</sub>(3) (30 nM). Sperm are loaded onto the micro scope and tracked for 10 s. A fluorescent image is acquired every second. The ratio value distributions of the test and control groups are compared.

### 2.5 Track, Trap (Constant Power and Constant Duration), and Fluorescently Image

Sperm labeled with DiOC<sub>2</sub>(3) are tracked and trapped under constant power (460 mW) for a constant duration (90 s). For each sperm analyzed, fluorescent images are acquired approximately once every second during the 5s prior to and after trapping and acquired continuously once the sperm is in the trap. Effects of prolonged exposure to the laser tweezers on MP and swimming speed (VCL in micrometers per second) are assessed.

### 2.6 Track, Trap (Decaying Laser Power), and Fluorescently Image

Sperm labeled with DiOC<sub>2</sub>(3) are tracked and trapped under decaying power. Again, for each sperm, fluorescent images are acquired once every second during the 5s prior to and post trapping and acquired continuously once the sperm is in the trap. Examples of the various sperm responses to the optical trap are described.

## 3 Results

### 3.1 Effect of Probe on Sperm Motility

The swimming speed (VCL in micrometers per second) distribution of sperm cells exposed to DiOC<sub>2</sub>(3) is compared to that of the control sperm using the Wilcoxon paired-sample test (the distributions are found not to be Gaussian, thus requiring the non-parametric test). The VCL distributions are found to be statistically equal, even when the probe is activated by the arc lamp (without arc lamp illumination;  $P > 0.3$ ,  $N_{\text{control}}=24$ ,  $N_{\text{DiOC}_2(3)}=37$ ; with arc lamp illumination;  $P > 0.2$ ,  $N_{\text{control}}=23$ ,  $N_{\text{DiOC}_2(3)}=19$ ). Thus, DiOC<sub>2</sub>(3) does not adversely affect sperm motility.

### 3.2 Sensitivity to Changes in MP

Since the probe used in this study is typically applied in flow cytometry experiments, we wanted to verify that our custom system and method of analysis is sensitive to changes in MP. We also wanted to verify that this probe reports changes in MP. Figure 2 shows the ratio value over a 10-s interval for sperm from the test group (with CCCP) and control group (without CCCP). The figure demonstrates that CCCP does indeed cause a decrease in MP



and that both the probe and the system are capable of reporting such a decrease. The average ratio value of sperm exposed to CCCP ( $3.74 \pm 0.75$ ,  $N_{\text{DiOC}_2(3)}=33$ ) versus that of the control sperm ( $5.82 \pm 0.41$ ,  $N_{\text{control}}=36$ ) is found to be statistically significantly different ( $P \ll 0.001$ ) using the Student's *T* test (distributions are found to be Gaussian). The velocity of each sperm was also measured. The average VCL value of sperm exposed to CCCP ( $67.15 \pm 20.77$ ) versus that of the control sperm ( $70.39 \pm 24.70$ ) is found to be statistically the same ( $P > 0.56$ ) using the Student's *T* test (distributions are found to be Gaussian).

### 3.3 Track, Trap (Constant Power and Constant Duration), and Fluorescently Image

Figure 3 shows the ratio value prior to trapping, during trap, and after trapping plotted over time for two different sperm. For the sperm in Fig. 3(a), there is an overall decline in ratio value over time as the sperm is held in the trap. Once released from the optical trap, the sperm's ratio value does increase, however, it does not fully recover within 5s to the original value it was prior to being trapped. Similarly, the sperm's swimming speed, VCL, does not recover to its pre-trapping value. For the sperm in Fig. 3(b), there is a slight decrease in ratio value while the sperm is in the trap. Again, neither swimming speed nor ratio value fully recover post trap to the pre-trapping values. A previous study had shown that trapping sperm for 15 s at a constant power of 420 mW in the focal volume had a negative effect on sperm motility.<sup>10</sup> The results reported here are consistent with those findings.

### 3.4 Track, Trap (Decaying Laser Power), and Fluorescently Image

Pesc was plotted against VCL (data not shown) and showed the same positive correlation between the two parameters as found in previous studies<sup>10</sup> (regressions applied to data sets found to be statistically equal,  $P > 0.2$ ). Figure 4 plots the ratio value over time for four sperm for the three different phases: prior to trapping, during trap, and after trapping. These four examples demonstrate the various responses the sperm have to the optical trap. The sperm in Fig. 4(a) did not escape the trap. After 10 s, the trapping power reaches the minimum 3.8 mW, at which point the trap turns off. This sperm's VCL slightly increased after being trapped, but the average ratio value decreased. The sperm in Fig. 4(b) escaped the trap at 55 mW and had an approximate 18% increase in VCL after trapping. However, the average ratio value was nearly the same after trapping as it was prior to trapping. The sperm in Fig. 4(c), although it escaped at a relatively high power, had a significant decrease in VCL, yet the average ratio value increased slightly. The sperm in Fig. 4(d), which escaped the trap at 26 mW, also had a decrease in VCL and an increase in average ratio value.

## 4 Discussion

In this paper, a mitochondrial membrane potential probe was used in combination with a custom-automated tracking and trapping system. We demonstrated how this technique can be applied to the study of sperm motility and energetics. Moreover, we created a protocol that can be used to compare various MP probes. First, the effects of the probe on sperm swimming speed are established. Specifically,  $\text{DiOC}_2(3)$  was shown to not affect sperm swimming speed (VCL). Second, the probe's ability to report an expected decrease in MP was verified. The ratio measurement of the red to green fluorescent signal from  $\text{DiOC}_2(3)$  showed a significant decrease in MP caused by the addition of the proton ionophore CCCP (see Fig. 2). This also demonstrates that the system's hardware and software, including the custom algorithms, are sensitive to changes in MP.

Third, the system can then be used to monitor MP of individual sperm over a long period of time and assess the adverse effects of prolonged exposure to optical traps. As shown in Fig. 3, both VCL and MP values post-trapping are less than those prior to trapping. These results

show that the ratio value can reflect the varying degrees of cell damage induced by the laser trap as well as partial cell recovery once the laser trap is turned off. Fourth, and finally, we have demonstrated how this system can be used to simultaneously measure sperm swimming speed, escape laser power, and sperm mitochondrial MP in real time.

In conclusion, we created a technique to quantitatively assess sperm quality and viability. We demonstrated how a combination of imaging and optical tools can be used to provide a detailed description of individual sperm by measuring not only sperm motility parameters, such as VCL and Pesc, but also mitochondrial MP. This system can therefore be used to address the relationship between mitochondrial respiration and motility. Knowing that there is indeed a relationship between VCL and Pesc, as found in a previous study,<sup>10</sup> one would expect that there would also be relationships between VCL and MP and/or Pesc and MP. However, to draw statistically significant conclusions regarding these relationships, more experiments must be conducted to achieve larger *N* values. More importantly, this system can be used to gain a better understanding of the role of oxidative phosphorylation in sperm cell motility. For example, the results found in this paper interestingly show no correlation between MP and sperm motility (in terms of VCL) when the sperm were exposed to CCCP. One would expect exposure to this ionophore would inhibit mitochondrial ATP production and thus reduce sperm motility. However, no such decrease in velocity was observed (the VCL of the control group was found to be statistically equal to that of the test group). This suggests that perhaps another pathway, such as glycolysis, which is known to occur along the sperm tail, or principal piece,<sup>24–26</sup> may be supporting motility when oxidative phosphorylation is inhibited. Future studies will assess the effects of various electron transport chain inhibitors, such as rotenone and antimycin A, as well as glycolytic inhibitors, such as 2-deoxy-D-glucose, on sperm mitochondrial MP, VCL, and Pesc.

## Acknowledgments

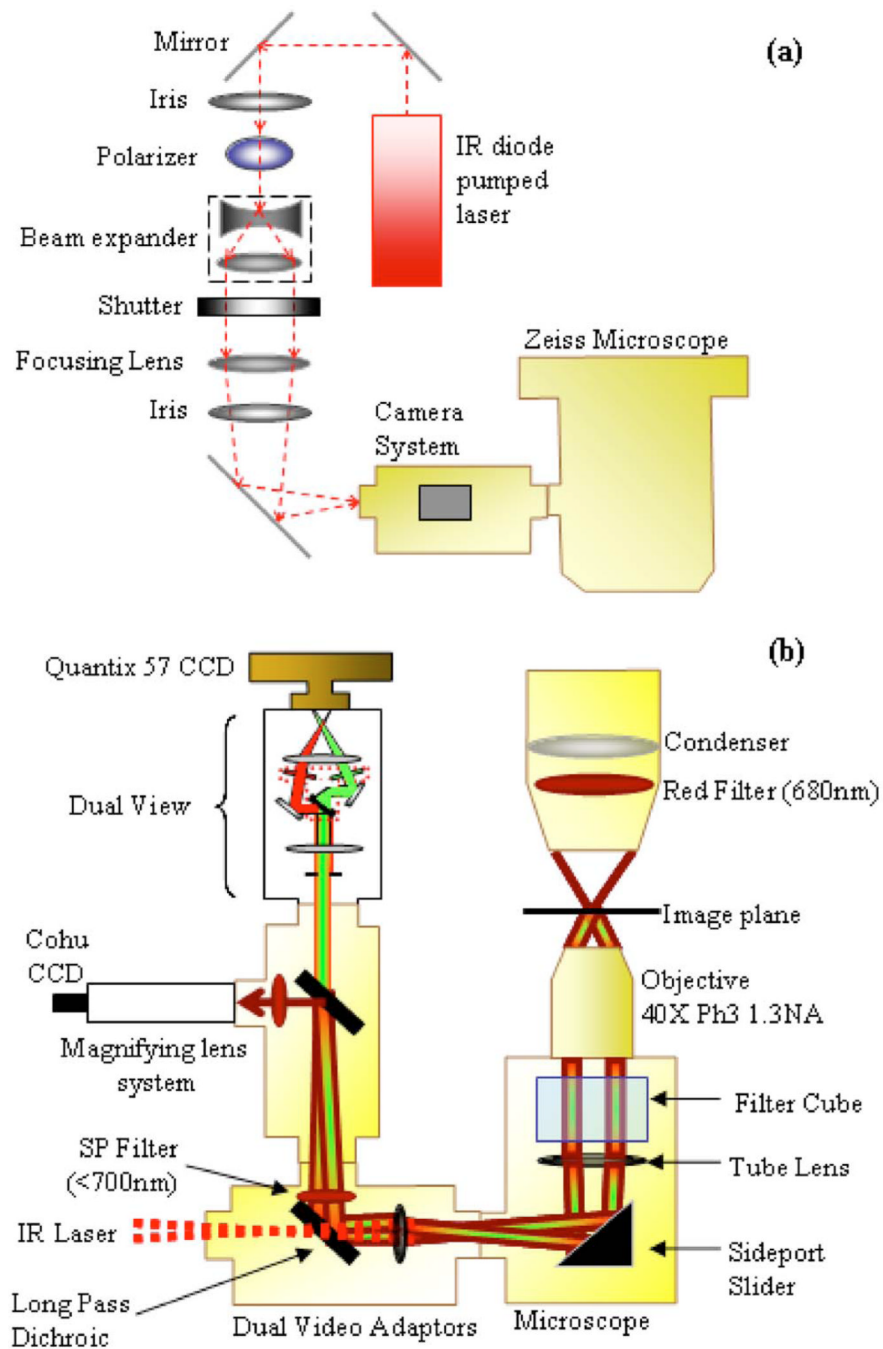
This work was supported by funds from the Beckman Laser Institute Inc. Foundation and a grant from the Air Force Office of Scientific Research (AFOSR No. F9620-00-1-0371) awarded to MWB.

## References

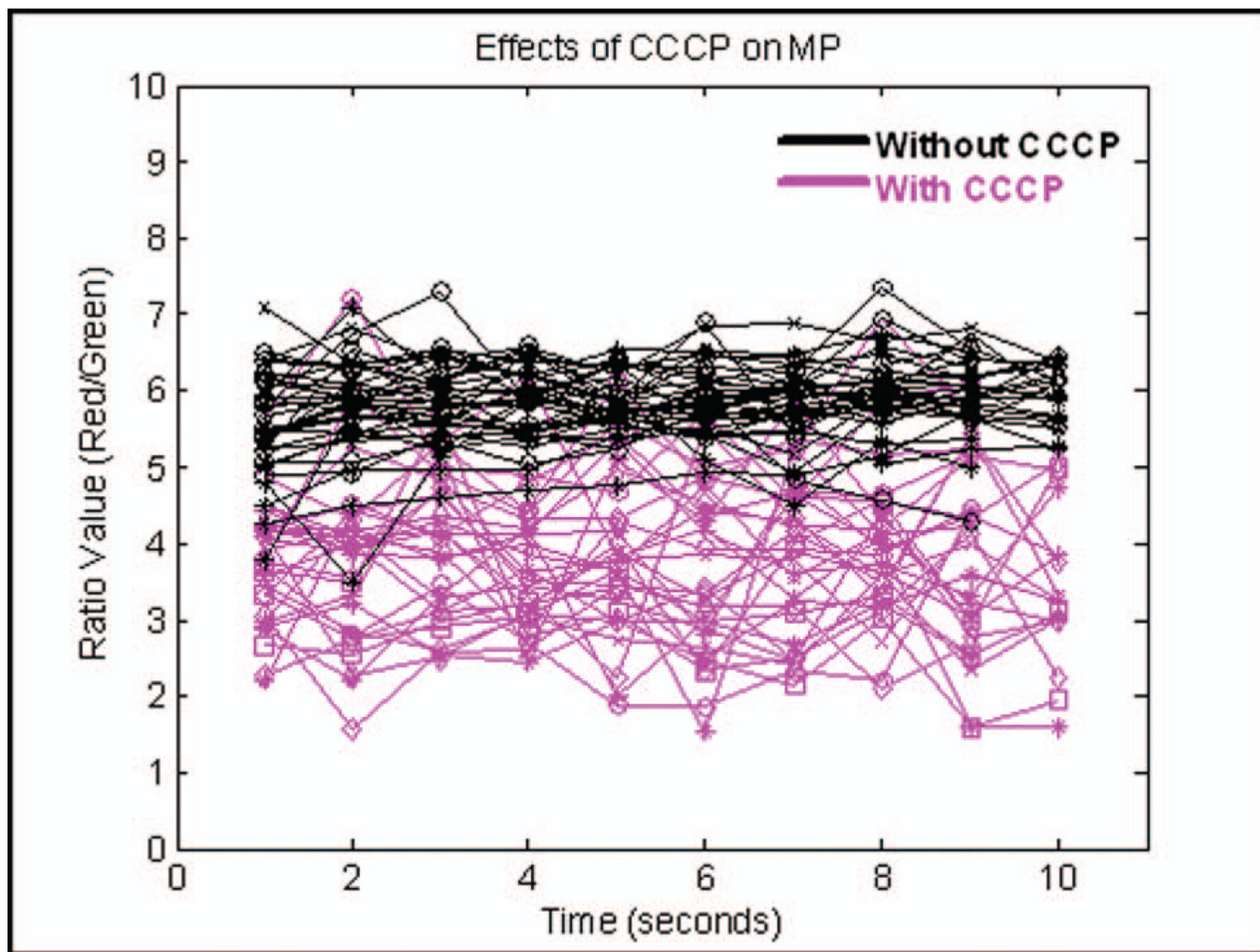
1. Amann RP, Katz DF. Reflections on CASA after 25 years. *J. Androl.* 2004; 25(3):317–325. [PubMed: 15064305]
2. Mortimer, D. *Practical Laboratory Andrology*. New York: Oxford University Press; 1994.
3. Marchetti C, Obert G, Deffosez A, Formstecher P, Marchetti P. Study of mitochondrial membrane potential, reactive oxygen species, DNA fragmentation and cell viability by flow cytometry in human sperm. *Hum. Reprod.* 2002; 17(5):1257–1265. [PubMed: 11980749]
4. Marchetti C, Jouy N, Leroy-Martin B, Deffosez A, Formstecher P, Marchetti P. Comparison of four fluorochromes for the detection of the inner mitochondrial membrane potential in human spermatozoa and their correlation with sperm motility. *Hum. Reprod.* 2004; 19(10):2267–2276. [PubMed: 15256505]
5. Gallon F, Marchetti C, Jouy N, Marchetti P. The functionality of mitochondria differentiates human spermatozoa with high and low fertilizing capability. *Fertil. Steril.* 2006; 86(5):1526–1530. [PubMed: 16996512]
6. Kasai T, Ogawa K, Mizuno K, Nagai S, Uchida Y, Ohta S, Fujie M, Suzuki K, Hirata S, Hoshi K. Relationship between sperm mitochondrial membrane potential, sperm motility, and fertility potential. *Asian J. Androl.* 2002; 4(2):97–103. [PubMed: 12085099]
7. Novo D, Perlmutter NG, Hunt RH, Shapiro HM. Accurate flow cytometric membrane potential measurement in bacteria using diethyloxycarbocyanine and a ratiometric technique. *Cytometry.* 1999; 35:55–63. [PubMed: 10554181]



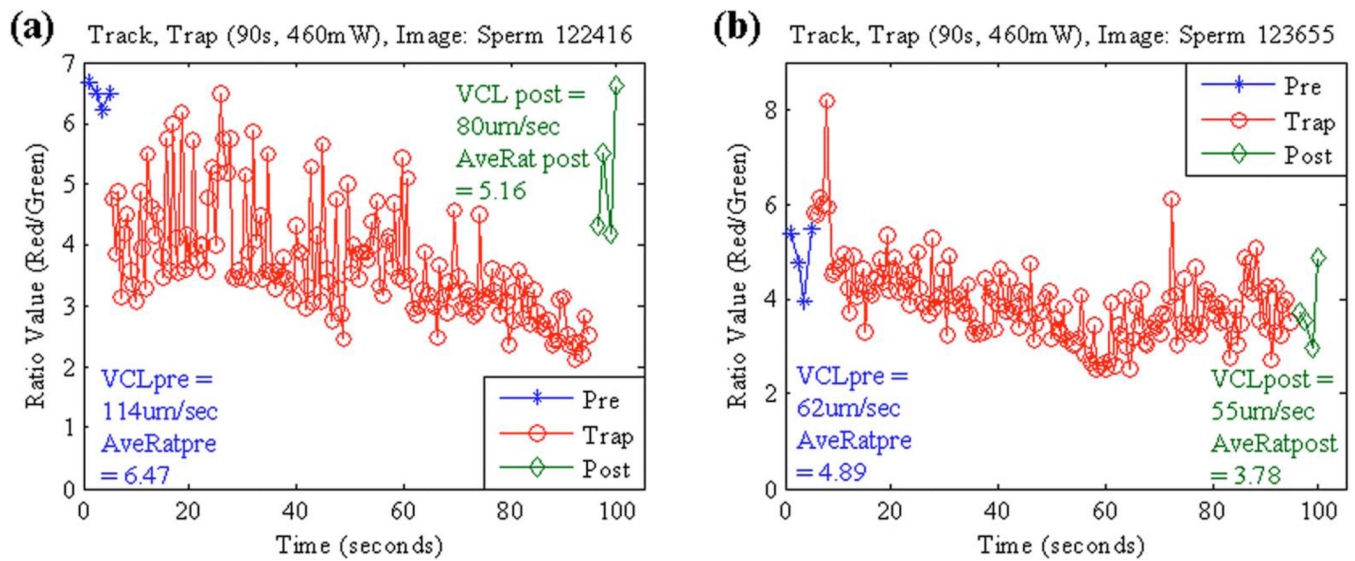
8. Konig K, Svaasand L, Liu Y, Sonek G, Patrizio P, Tadir Y, Berns MW, Tromberg BJ. Determination of motility forces of human spermatozoa using an 800 nm optical trap. *Cell. Mol. Biol. (Paris)*. 1996; 42(4):501–509.
9. Tadir Y, Wright WH, Vafa O, Ord T, Asch RH, Berns MW. Force generated by human sperm correlated to velocity and determined using a laser generated optical trap. *Fertil. Steril.* 1990; 53(5): 944–947. [PubMed: 2332067]
10. Nascimento JM, Botvinick EL, Shi LZ, Durrant B, Berns MW. Analysis of sperm motility using optical tweezers. *J. Biomed. Opt.* 2006; 11(4):044001. [PubMed: 16965158]
11. Nascimento JM, Shi LZ, Meyers S, Gagneux P, Loskutoff NM, Botvinick EL, Berns MW. The use of optical tweezers to study sperm competition and motility in primates. *J.R. Soc., Interface*. 2007; 5(20):297–302. [PubMed: 17650470]
12. Mei A, Botvinick E, Berns MW. Monitoring sperm mitochondrial respiration response in a laser trap using ratiometric fluorescence. *Proc. SPIE*. 2005; 5930(2F):1–11.
13. Shi LZ, Nascimento J, Berns MW, Botvinick E. Computer-based tracking of single sperm. *J. Biomed. Opt.* 2006; 11(5):054009. [PubMed: 17092158]
14. Shi LZ, Nascimento JM, Chandsawangbhuwana C, Berns MW, Botvinick E. Real-time automated tracking and trapping system (RATTS). *Microsc. Res. Tech.* 2006; 69(11):894–902. [PubMed: 16892192]
15. Shi LZ, Botvinick EL, Nascimento J, Chandsawangbhuwana C, Berns MW. A real-time single sperm tracking, laser trapping, and ratiometric fluorescent imaging system. *Proc. SPIE*. 2006; 6326:63260x.
16. Durrant BS, Harper D, Amodeo A, Anderson A. Effects of freeze rate on cryosurvival of domestic dog epididymal sperm. *J Androl.* 2000; 21(Suppl 59)
17. Harper SA, Durrant BS, Russ KD, Bolamba D. Cryo-preservation of domestic dog epididymal sperm: a model for the preservation of genetic diversity. *J Androl.* 1998; 19(Suppl 50)
18. Dantas ZN, Araujo E Jr, Tadir Y, Berns MW, Schell MJ, Stone SC. Effect of freezing on the relative escape force of sperm as measured by a laser optical trap. *Fertil. Steril.* 1995; 63(1):185–188. [PubMed: 7805910]
19. Biggers, JD.; Whitten, WD.; Whittingham, DG. The culture of mouse embryos *in vitro*. In: Daniel, JC., Jr, editor. *Methods of Mammalian Embryology*. San Francisco: Freeman; 1971. p. 86-116.
20. Bedu-Addo K, Lefievre L, Moseley FLC, Barratt CLR, Publicover SJ. Bicarbonate and bovine serum albumin reversibly ‘switch’ capacitation-induced events in human spermatozoa. *Mol. Hum. Reprod.* 2005; 11(9):683–691. [PubMed: 16192296]
21. Novo D, Perlmutter NG, Hunt RH, Shapiro HM. Multi-parameter flow cytometric analysis of antibiotic effects on membrane potential, membrane permeability, and bacterial counts of *Staphylococcus aureus* and *Micrococcus luteus*. *Antimicrob. Agents Chemother.* 2000; 44(4):827–834. [PubMed: 10722477]
22. Guzman-Grenfell AM, Bonilla-Hernandez MA, Gonzalez-Martinez MT. Glucose induces a  $Na^+$ ,  $K^+$ -ATPase-dependent transient hyperpolarization in human sperm. I. Induction of changes in plasma membrane potential by the proton ionophore CCCP. *Biochim. Biophys. Acta.* 2000; 1464:188–198. [PubMed: 10727606]
23. Liaw LH, Berns MW. Electron microscope autoradiography on serial sections of preselected single living cells. *J. Ultrastruct. Res.* 1981; 75:187–194. [PubMed: 6167738]
24. Turner RM. Tales from the tail: what do we really know about sperm motility. *J Androl.* 2003; 24(6):790–803. [PubMed: 14581499]
25. Ford WCL. Glycolysis and sperm motility: does a spoonful of sugar help the flagellum go round. *Hum. Reprod. Update.* 2006; 12(3):269–274. [PubMed: 16407453]
26. Mukai C, Okuno M. Glycolysis plays a major role for adenosine triphosphate supplementation in mouse sperm flagellar movement. *Biol. Reprod.* 2004; 71:540–547. [PubMed: 15084484]



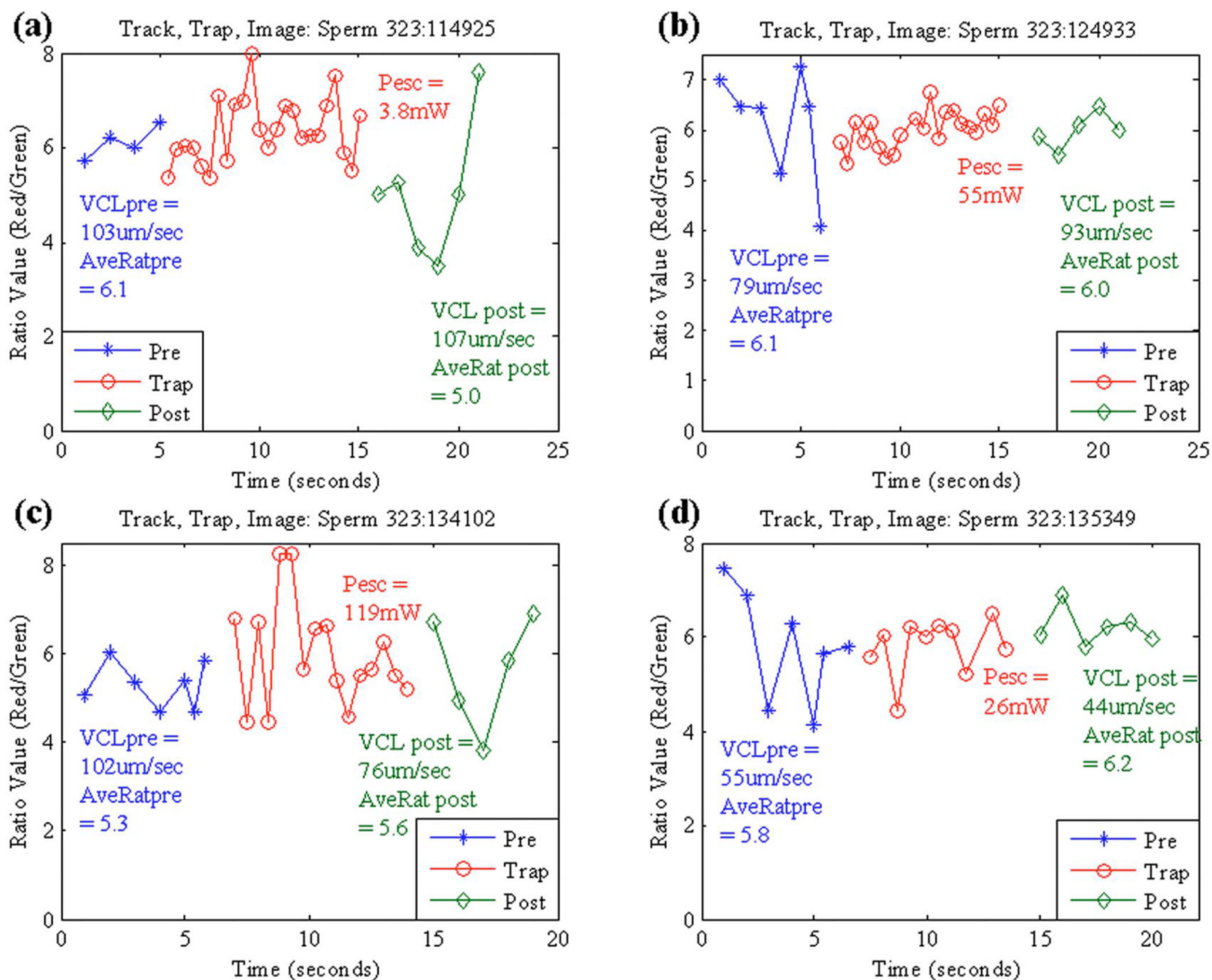
**Fig. 1.** (a) Optical schematic showing the optical components used to generate and control the laser tweezers and (b) imaging setup showing the illumination sources, filters, and cameras used to image the sperm in both phase contrast and fluorescence.



**Fig. 2.** Effects of CCCP on mitochondrial membrane potential. The ratio value (red/green fluorescence) is plotted against time (in seconds). Ratio values are measured over a 10-s interval for test sperm group (with CCCP, in magenta) and control sperm group (without CCCP, in black). Each track represents an individual sperm.



**Fig. 3.** Track, trap (constant power, constant duration) and fluorescently image. The ratio value (red/green) is plotted against time (in seconds) for the three different phases: prior to trapping, during trap, and after trapping. Both the average ratio value (AveRat) and VCL prior to (pre) and after trapping (post) are inset in the figure for each sperm (a) and (b). A trap duration of 90 s has a negative effect on sperm motility and energetics. (Color online only.)

**Fig. 4.**

Track, trap (decaying laser power) and fluorescently image. The ratio value (red/green) is plotted against time (in seconds) for the three different phases: prior to trapping, during trap, and after trapping. Various escape powers and swimming speeds are represented by the four sperm. The average ratio value (AveRat) and VCL prior to (pre) and after trapping (post), as well as Pesc, are inset in the figure for each sperm (a) to (d). (Color online only.)